

# Dinuclear Ruthenium(II) Polypyridyl Complexes Containing Large, Redox-Active, Aromatic Bridging Ligands: Synthesis, Characterization, and Intramolecular Quenching of MLCT Excited States

Mahn-Jong Kim,<sup>†</sup> Rama Konduri,<sup>†</sup> Hongwei Ye,<sup>†,‡</sup> Frederick M. MacDonnell,<sup>\*,†</sup> Fausto Puntoriero,<sup>§</sup> Scolastica Serroni,<sup>§</sup> Sebastiano Campagna,<sup>\*,§</sup> Tina Holder,<sup>†</sup> Gary Kinsel,<sup>†</sup> and Krishnan Rajeshwar<sup>†</sup>

Department of Chemistry and Biochemistry, University of Texas at Arlington, Arlington, Texas 76019, and Dipartimento di Chimica Inorganica, Chimica Analitica e Chimica Fisica, University of Messina, Via Sperone 31, I-98166 Messina, Italy

Received October 3, 2001

Two new ruthenium(II) polypyridyl dimers containing the large planar aromatic bridging ligands 9,11,20,22-tetraazatetrapyrido[3,2-*a*:2'3'-*c*:3'',2''-*t*:2''',3''''-*n*]pentacene (tatpp) and 9,11,20,22-tetraazatetrapyrido[3,2-*a*:2'3'-*c*:3'',2''-*t*:2''',3''''-*n*]pentacene-10,21-quinone (tatpq) have been synthesized and characterized by <sup>1</sup>H and <sup>13</sup>C NMR, MALDI mass spectrometry, and elemental analyses. The electronic properties (UV–vis, redox, photophysical) of these dimers are analyzed in the context of orbital calculations (PM3 level) on the bridging ligands. A localized orbital model is proposed in which low-lying acceptor orbitals on the center portion of the ligands effectively quench the Ru(II)-based MLCT emission via a mechanism that can be viewed as intramolecular electron transfer to specific subunits of the bridges.

## Introduction

Oligonuclear complexes made by Ru(II) and Os(II) polypyridine components have been extensively investigated because they play key roles in the development of multi-component (supramolecular) artificial systems for photochemical energy conversion and other related photonic devices.<sup>1</sup> In the design of such systems, the bridging ligands used to connect two or more metal polypyridine subunits are crucial because they (i) allow the assembly of the metal subunits in a topologically (and sometimes also configurationally) controlled fashion (structural role) and (ii) can afford

electronic coupling between the linked partners to allow, in turn, intercomponent energy and/or electron-transfer processes (functional role).<sup>1c</sup> However, bridging ligands containing within their own structure subunits that themselves play active roles in photoinduced energy and/or electron transfer are rare.<sup>2</sup>

Here we report the synthesis, absorption spectra, photophysical properties, and redox behavior of two new dinuclear Ru(II) polypyridine complexes containing novel large aromatic bridging ligands and demonstrate that specific subunits of the large bridging ligands play important roles for determining the photophysical and redox properties of the new species. The new compounds are [(phen)<sub>2</sub>Ru(tatpp)Ru(phen)<sub>2</sub>]<sup>4+</sup> (**1**) and [(phen)<sub>2</sub>Ru(tatpq)Ru(phen)<sub>2</sub>]<sup>4+</sup> (**2**) (phen = 1,10-phenanthroline; structures of the tatpp and tatpq ligands are shown in Figure 1). PM3 calculations of HOMO and LUMOs bridging ligands are also presented. The results indicate that the intrinsically luminescent MLCT excited states of the (phen)<sub>2</sub>Ru(phen')<sup>2+</sup> subunits (phen' here repre-

\* To whom correspondence should be addressed. E-mail: macdonn@uta.edu (F.M.M.); photochem@chem.unime.it (S.C.).

<sup>†</sup> University of Texas at Arlington.

<sup>‡</sup> Deceased.

<sup>§</sup> University of Messina.

(1) (a) Balzani, V.; Scandola, F. *Supramolecular Chemistry*; Horwood: Chichester, U.K., 1991. (b) Hagfeldt, A.; Graetzel, M. *Chem. Rev.* **1995**, *95*, 49. (c) Balzani, V.; Juris, A.; Venturi, M.; Campagna, S.; Serroni, S. *Chem. Rev.* **1996**, *96*, 759. (d) Harriman, A.; Ziessel, R. *Chem. Commun.* **1996**, 1707. (e) Bignozzi, C. A.; Schoonover, J. R.; Scandola, F. *Prog. Inorg. Chem.* **1997**, *44*, 1. (f) De Cola, L.; Belser, P. *Coord. Chem. Rev.* **1998**, *177*, 301. (g) Collin, J.-P.; Gaviña, P.; Heitz, V.; Sauvage, J.-P. *Eur. J. Inorg. Chem.* **1998**, 1. (h) Balzani, V.; Campagna, S.; Denti, G.; Juris, A.; Serroni, S.; Venturi, M. *Acc. Chem. Res.* **1998**, *31*, 26. (i) Barigelletti, F.; Flamigni, L. *Chem. Soc. Rev.* **2000**, *29*, 1.

(2) (a) Belser, P.; Dux, R.; Baak, M.; De Cola, L.; Balzani, V. *Angew. Chem., Int. Ed. Engl.* **1995**, *34*, 595. (b) Encinas, S.; Barthram, A. M.; Ward, M. D.; Barigelletti, F.; Campagna, S. *Chem. Commun.* **2001**, 277. (c) López, R.; Leiva, A. M.; Zuloaga, F.; Loeb, B.; Norambuena, E.; Omberg, K. M.; Schoonover, J. R.; Striplin, D.; Devenney, M.; Meyer, T. J. *Inorg. Chem.* **1999**, 2924–2930

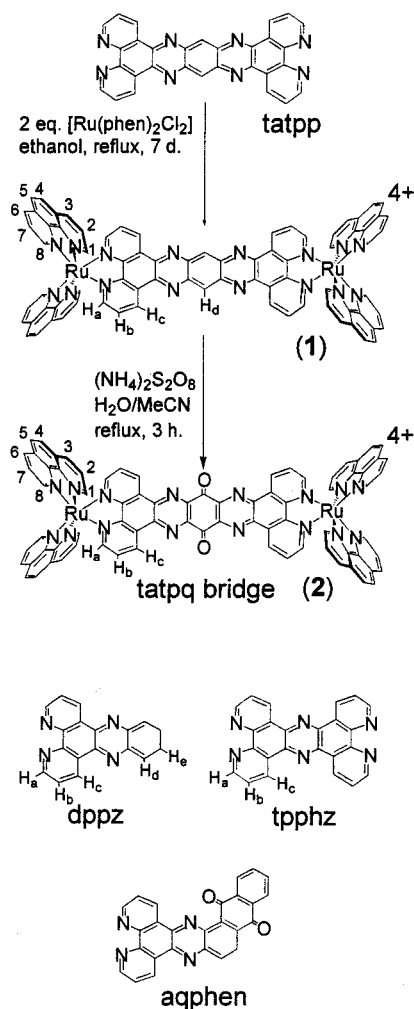


**Figure 1.** Synthesis and structural formulas of complexes **1** and **2**. Structures of related tpphz and dppz ligands are shown for comparison.

sents the phenanthroline moiety of the bridging ligand) in both complexes are efficiently quenched by the central moieties of the bridges, most likely by oxidative electron transfer.

## Experimental Section

**Chemicals.** The compounds 1,10-phenanthroline (phen), 1,2,4,5-benzenetetramine tetrahydrochloride, and hydrated ruthenium(III)-chloride were purchased from Aldrich or Alfa and used without further purification. 1,10-Phenanthroline-5,6-dione (phendione)<sup>3</sup> and  $[\text{Ru}(\text{phen})_2(\text{phendione})]\text{Cl}_2$ <sup>4</sup> were prepared according to literature procedures. All organic solvents were of analytical grade and used as received.

**Physical Measurements.** <sup>1</sup>H and <sup>13</sup>C NMR spectra were obtained on a Bruker MSL-300 or JEOL Eclipse Plus 500 MHz spectrometer using CD<sub>3</sub>CN as the solvent unless otherwise noted. Chemical shifts are given in ppm and referenced to TMS. FTIR spectra were obtained on KBr pellets using a Bruker Vector 22 spectrometer. MALDI mass spectra were obtained as described previously for related complexes.<sup>5</sup> UV–visible spectra were obtained on a Hewlett-Packard HP8453A spectrophotometer in MeCN. Cyclic

voltammetry (CV) and differential pulse voltammetry (DPV) were made on a CH Instruments (1620A) electrochemical workstation using a glassy carbon working electrode, platinum wire counter electrode, and a Ag/AgCl or SCE reference electrode. All potentials are reported versus SCE. Measurements were performed in degassed (N<sub>2</sub>) acetonitrile solutions of **1** and **2** (0.5 mM) using Bu<sup>n</sup><sub>4</sub>NPF<sub>6</sub> (0.1 M) as the supporting electrolyte. Ligand geometry optimizations and MO calculations were performed using MacSpartan Pro (V. 1.0.2, Wavefunction, Inc., Irvine, CA) at the PM3 level.

**Syntheses. 9,11,20,22-Tetraazatetrapyrido[3,2-*a*:2'3'-*c*:3'',2''-1:2''',3'''-*n*]pentacene (tatpp).** A mixture of phendione (0.50 g, 2.4 mmol), 1,2,4,5-benzenetetramine tetrahydrochloride (0.338 g, 1.19 mmol), and potassium carbonate (0.329 g, 2.38 mmol) was suspended in ethanol (15 mL) and refluxed under nitrogen for 12 h. After cooling of the reaction to room temperature, the precipitate was filtered out, washed with 15 mL of hot water (3×) and 15 mL of boiling ethanol (3×), and dried in vacuo at 60 °C. Yield: 0.41 g (70%). Anal. Calcd for C<sub>30</sub>H<sub>14</sub>N<sub>8</sub>·1.5H<sub>2</sub>O: C, 70.17; H, 3.34; N, 21.82. Found: C, 69.77; H, 2.95; N, 21.82. <sup>1</sup>H NMR (300 MHz, CDCl<sub>3</sub>:CF<sub>3</sub>COOD = 90:10; δ, ppm): 10.20 (d, *J* = 8.0 Hz, 4H), 9.79 (s, 2H), 8.33 (d, *J* = 4.0 Hz, 4H), 8.36 (dd, *J*<sub>1</sub> = 7.3 Hz, *J*<sub>2</sub> = 4.5 Hz, 4H). EI MS: *m/z* 486.7.

**[(phen)<sub>2</sub>Ru(tatpp)Ru(phen)<sub>2</sub>][PF<sub>6</sub>]<sub>4</sub> (**1**).** A mixture of tatpp (0.1 g, 0.02 mmol) and Ru(phen)<sub>2</sub>Cl<sub>2</sub> (0.26 g, 0.05 mmol) was suspended in ethanol (30 mL) and water (30 mL) and refluxed for 7 days under N<sub>2</sub> atmosphere. After reflux, the solution was allowed to stand for 12 h at 4 °C. The solution was filtered and the product precipitated by addition of aqueous NH<sub>4</sub>PF<sub>6</sub> to the supernatant. The precipitate was filtered out and washed with 10 mL of water (3×) and 10 mL of ethanol. The crude product was further purified by repeated (3×) metatheses between the Cl<sup>−</sup> and PF<sub>6</sub><sup>−</sup> salts. The chloride salt was prepared from the hexafluorophosphate salt by dissolving the complex in a minimum amount of acetone and adding a concentrated solution of Bu<sup>n</sup><sub>4</sub>NCl in acetone. The resulting precipitate was filtered out and washed with 5 mL of acetone (3×) and 10 mL of diethyl ether. The hexafluorophosphate salt was prepared from the chloride form by dissolving the complex in a minimum amount of water and adding a concentrated solution of ammonium hexafluorophosphate. The resulting precipitate was filtered out and washed with 10 mL of water (3×), 10 mL of ethanol, and 10 mL of diethyl ether. Yield (PF<sub>6</sub><sup>−</sup> salt): 0.27 g (65%). Anal. Calcd for C<sub>78</sub>H<sub>46</sub>N<sub>16</sub>Ru<sub>2</sub>P<sub>4</sub>F<sub>24</sub>: C, 47.07; H, 2.33; N, 11.27. Found: C, 47.12; H, 2.86; N, 11.57. <sup>1</sup>H NMR (δ, 500 MHz, MeCN-*d*<sub>6</sub>): 9.70 (d, *J* = 8.3 Hz, 4H), 8.65 (dd, *J*<sub>1</sub> = 12.8 Hz, *J*<sub>2</sub> = 8.3 Hz, 8H), 8.30 (d, *J* = 5.0 Hz, 4H), 8.30 (s, 8H), 8.26 (s, 2H), 8.15 (d, *J* = 5.5 Hz, 4H), 8.03 (d, *J* = 5.5 Hz, 4H), 7.82 (dd, *J*<sub>1</sub> = 7.8 Hz, *J*<sub>2</sub> = 5.5 Hz, 4H), 7.72 (dd, *J*<sub>1</sub> = 8.3 Hz, *J*<sub>2</sub> = 5.1 Hz, 4H), 7.66 (*J*<sub>1</sub> = 8.3 Hz, *J*<sub>2</sub> = 5.5 Hz, 4H). <sup>13</sup>C NMR (δ, 125 MHz, MeCN-*d*<sub>6</sub>): 155.97, 154.22, 153.86, 153.11, 148.75, 148.66, 143.90, 142.21, 137.98, 137.90, 134.79, 132.01, 131.99, 131.66, 131.38, 129.02, 128.99, 128.59, 126.88 and 126.82. MALDI MS: *m/z* 1698 ([**1** − 2PF<sub>6</sub>]<sup>+</sup>), 1557 ([**1** − 3PF<sub>6</sub>]<sup>+</sup>), 1411 ([**1** − 4PF<sub>6</sub>]<sup>+</sup>).

**[(phen)<sub>2</sub>Ru(tatpq)Ru(phen)<sub>2</sub>][PF<sub>6</sub>]<sub>4</sub> (**2**).** A mixture of [Ru<sub>2</sub>(phen)<sub>4</sub>(tatpp)][PF<sub>6</sub>]<sub>4</sub> (30 mg, 0.015 mmol) and (NH<sub>4</sub>)<sub>2</sub>S<sub>2</sub>O<sub>8</sub> (17 mg, 0.08 mmol) was dissolved in 5 mL of acetonitrile and 5 mL of water, which was refluxed for 3 h under N<sub>2</sub> atmosphere. After cooling, the solution was filtered and the supernatant reduced to half-volume under the reduced pressure. The crude product was precipitated by addition of a concentrated aqueous solution of NH<sub>4</sub>PF<sub>6</sub> and then isolated by filtration and washed with 10 mL

(3) Yamada, M.; Tanaka, Y.; Yoshimoto, Y.; Kuroda, S.; Shimao, I. *Bull. Chem. Soc. Jpn.* **1992**, *65*, 1006–1011.

(4) Hiort, C.; Lincoln, P.; Nordén, B. *J. Am. Chem. Soc.* **1993**, *115*, 3448–3454.

(5) Bodige, S.; Torres, A. S.; Maloney, D. J.; Tate, D.; Walker, A.; Kinsel, G.; MacDonnell, F. M. *J. Am. Chem. Soc.* **1997**, *117*, 110364–10369.

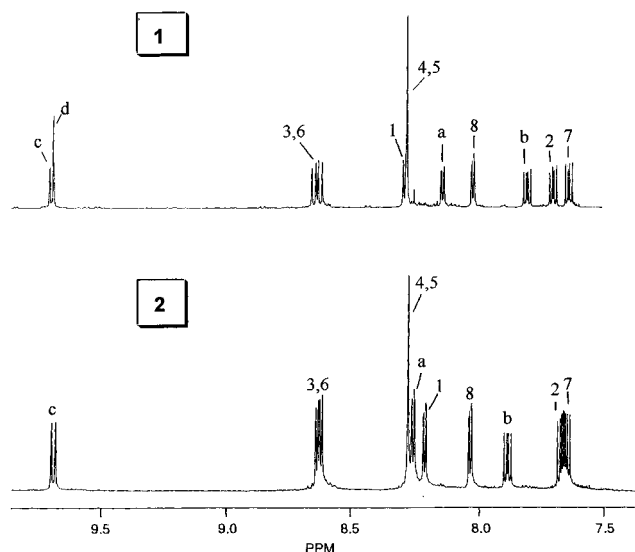


**Figure 2.**  $^1\text{H}$ NMR spectra (500 MHz) of the hexafluorophosphate salts of **1** (top) and **2** (bottom) in  $\text{MeCN-}d_3$ . (Numbering scheme is shown in Figure 1.)

water (3 $\times$ ). This solid was dissolved in acetonitrile, filtered, and precipitated by addition of a concentrated solution of  $\text{NH}_4\text{PF}_6$  in ethanol. The reddish-orange product was isolated by filtration, washed with 10 mL of ethanol–water (1:1), and dried in vacuo at 60  $^\circ\text{C}$ . Yield: 25 mg (83%). Anal. Calcd for  $\text{C}_{78}\text{H}_{44}\text{N}_{16}\text{O}_2\text{-Ru}_2\text{P}_4\text{F}_{24}$ : C, 46.40; H, 2.20; N, 11.10. Found: C, 46.86; H, 2.63; N, 10.72.  $^1\text{H}$  NMR ( $\delta$ , 500 MHz,  $\text{MeCN-}d_6$ ): 9.68 (d,  $J = 8.1$  Hz, 4H), 8.64 (dd,  $J_1 = 9.3$  Hz,  $J_2 = 5.6$  Hz, 8H), 8.28 (s, 8H), 8.27 (d,  $J = 5.4$  Hz, 4H), 8.23 (d,  $J = 5.1$  Hz, 4H), 8.04 (d,  $J = 5.2$  Hz, 4H), 7.88 (dd,  $J_1 = 7.8$  Hz,  $J_2 = 5.6$  Hz, 4H), 7.68 (dd,  $J_1 = 8.3$  Hz,  $J_2 = 5.1$  Hz, 4H), 7.65 ( $J_1 = 8.3$  Hz,  $J_2 = 5.1$  Hz, 4H).  $^{13}\text{C}$  NMR ( $\delta$ , 500 MHz,  $\text{MeCN-}d_6$ ): 179.36, 156.79, 154.26, 153.91, 152.38, 148.72, 148.66, 146.02, 143.90, 137.99, 137.94, 135.16, 132.01, 131.98, 130.54, 128.99, 128.55, 128.86 and 126.80. FTIR (KBr pellet): 1704.8  $\text{cm}^{-1}$  (C=O stretching). MALDI MS:  $m/z$  1734 ( $[\text{2} - 2\text{PF}_6]^+$ ), 1591 ( $[\text{2} - 3\text{PF}_6]^+$ ), 1446 ( $[\text{2} - 4\text{PF}_6]^+$ ).

## Results and Discussion

As shown in Figure 1, complex **1** is readily prepared from the reaction of 2 equiv of  $[\text{Ru}(\text{phen})_2\text{Cl}_2]$  with the free tatpp ligand; however, the reaction requires long reflux periods (7 days reflux) due to the sparingly soluble nature of the uncoordinated tatpp ligand. Somewhat surprisingly, this complex is very sensitive to decomposition and is difficult to purify by column chromatography (silica or alumina) without destroying the sample. For this reason, we have deliberately avoided the column purification procedures typical of this class of compounds. Repeated metatheses, as described above, were required to obtain an analytically pure product. The tatpq-bridged dimer **2** was significantly easier to prepare and was considerably more robust. Oxidation of **1** with a slight excess of ammonium peroxydisulfate in acetonitrile/water (1:1) cleanly gives **2** in 83% yield.

Both complexes **1** and **2** have been thoroughly characterized by elemental analyses,  $^1\text{H}$  NMR,  $^{13}\text{C}$  NMR, and mass spectrometry. The  $^1\text{H}$  NMR spectra of the two dimers are shown in Figure 2, and the signals have been assigned by COSY analyses and via comparison with the spectra of the

related tpphz-bridged dimers,  $[(\text{phen})_2\text{Ru}(\text{tpphz})\text{Ru}(\text{phen})_2]^{4+}$  (**3**; for structure of tpphz, see Figure 1). As observed with numerous tpphz-bridged complexes,<sup>5–7</sup> the diastereomers of **1** and **2** are indistinguishable by NMR as a result of the large distances between the stereocenters. This is not surprising considering that the Ru–Ru distances in the tpphz complexes are 12.6  $\text{Å}$ <sup>8</sup> and are estimated at 17.5  $\text{Å}$  for the tatpp and tatpq dimers. All of the stereoisomers are high-symmetry species ( $D_2$  or  $C_{2h}$  point group), and only 12 of the 46 H signals are expected for **1** and 11 of 44 for **2**. One less than the expected number of peaks (11 for **1** and 10 for **2**) are observed (Figure 2). The large singlet at 8.30 ppm for **1** and 8.28 ppm for **2** is assigned to both  $\text{H}_4$  and  $\text{H}_5$ , which are magnetically equivalent under these conditions as has been reported for tpphz complexes of this type.<sup>5,7</sup> Otherwise, the  $^1\text{H}$  NMR spectra of **1** and **2** are similar except that the singlet at 9.69 ppm (overlapping with the doublet for  $\text{H}_c$ ) is missing in the spectrum of **2**. This peak is assigned to the central benzene hydrogens ( $\text{H}_d$ ) on **1**, and thus, it is expected that this peak should be absent in **2**.

The large downfield shift for  $\text{H}_d$  is surprising in that this degree of deshielding has only been observed for hydrogens such as  $\text{H}_c$ , which are both adjacent to and pointing over the nitrogen lone pairs of the pyrazine ring. For example, consider the relative deshielding observed for the dppz  $\text{H}_c$  and  $\text{H}_d$  (see Figure 1) in  $[(\text{phen})_2\text{Ru}(\text{dppz})]^{2+}$ , which are observed at 9.69 and 8.50 ppm, respectively.<sup>9</sup> In the present case, the large downfield shift for  $\text{H}_d$  (in **1**) must be a consequence of its position between two such pyrazine rings.

Analysis of the  $^{13}\text{C}$  NMR spectrum **1** and **2** shows one less aromatic type carbon in the 120–158 ppm region upon oxidation of **1** to **2** and a single new peak appearing at 179.4 ppm consistent with the formation of a carbonyl group. Placement of the quinone moiety on the central benzene ring is deduced from the simplicity of the  $^1\text{H}$  NMR spectrum, which is a clear result of the high symmetry of the tatpq complex. As expected for the quinone species, complex **2** has a strong carbonyl absorption at 1705  $\text{cm}^{-1}$  in the FTIR spectrum (which is not present in **1**).

The MALDI mass spectra of both **1** and **2** show peaks for the parent ion complexes minus two, three, or all four hexafluorophosphate anions. Surprisingly, only the peaks for the singly charged complexes are observed (i.e.  $[\text{M} - 2\text{PF}_6]^+$ ,  $[\text{M} - 3\text{PF}_6]^+$ , and  $[\text{M} - 4\text{PF}_6]^+$ ), which indicates that the complexes must be reduced to varying degrees during the MALDI ionization procedure (similar behavior has been observed in the MALDI mass spectra of related dendrimeric complexes<sup>5</sup>). Ion formation in MALDI typically results from protonation of the parent molecule during the laser/desorption

(6) Campagna, S.; Serroni, S.; Bodige, S.; MacDonnell, F. M. *Inorg. Chem.* **1999**, *38*, 692–701.

(7) (a) MacDonnell, F. M.; Ali, M. M.; Kim, M.-J. *Comments Inorg. Chem.* **2000**, *22*, 203. (b) Kim, M.-J.; MacDonnell, F. M.; Gimon-Kinsel, M. E.; DuBois, T.; Asgharian, N.; Griener, J. C. *Angew. Chem., Int. Ed.* **2000**, *39*, 615. (c) MacDonnell, F. M.; Bodige, S. *Inorg. Chem.* **1996**, *35*, 5758.

(8) Bolger, J.; Gourdon, A.; Ishow, E.; Launay, J.-P. *J. Chem. Soc., Chem. Commun.* **1995**, 1799.

(9) Amouyal, E.; Homsil, A.; Chambron, J.-C.; Sauvage, J.-P. *J. Chem. Soc., Dalton. Trans.* **1990**, 1841–1845.

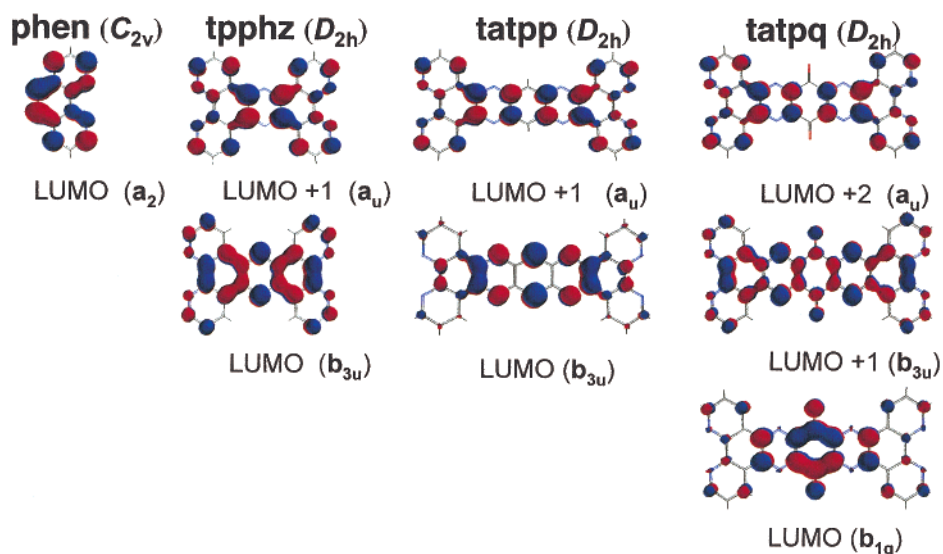


**Figure 3.** MO Pictures for the relevant orbitals in phen, tpphz, tatpp, and tatpq.

event to yield singly charged parent molecules 1 Da higher in mass. To obtain a singly charged  $[M - 2PF_6]^+$  ion, the molecule must either be reduced by two electrons and then protonated or reduced by a single electron leaving a residual single positive charge. Similar arguments can be made for the other complexes. Unfortunately the details of the ionization mechanism cannot be ascertained due to the poor resolution of the MALDI mass spectra which precludes mass assignment for the singly charged complexes to better than  $\pm 4$  Da. Regardless, the parent ion peaks for **2** are 33–35 amu greater than the corresponding peaks for **1**, which, in this context, is consistent with the addition of two oxygen atoms. Taken together, the NMR, IR, and mass spectrometric data offer complimentary results which clearly reveal the structures of **1** and **2**.

In view of the presence of the redox active quinone moiety on the tatpq ligand, and the complete lack of luminescence for either complex at room temperature in MeCN solution or at 77 K in a frozen matrix (vide infra), we decided to examine the molecular orbital (MO) structure of these bridging ligands. MO calculations were performed on the bridging ligands at the PM3 level. For comparison, the same calculations were also performed on phen and tpphz. The relevant orbitals, their signs, and electron density distributions and symmetry designations are presented in Figure 3. An orbital energy diagram showing the relative energies of these MOs with respect to one another is shown in Figure 4. Obviously, the results obtained from these calculations on the free ligands should be considered with caution when discussing the properties of the complexes; however, perturbations resulting from complexation are expected to be relatively constant across the series of ligands. In this sense, these calculations provide a valuable first approximation to the orbital structure of these  $\pi$ -acceptor ligands and qualitatively afford orbital energies which have relative, rather than absolute, values.

The most important trends from these calculations concern the similarity of certain orbitals across the series of ligands. As seen in Figure 3, the orbitals in each row are all related

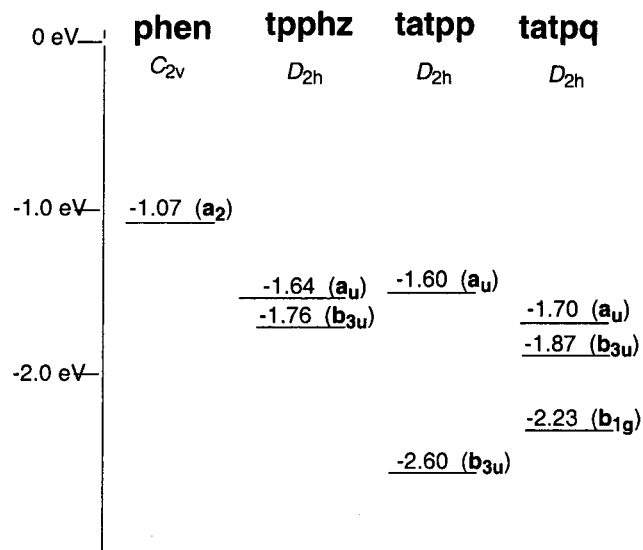


**Figure 4.** MO energy diagram of the relevant LUMOs for the phen, tpphz, tatpp, and tatpq ligands.

by both symmetry and orbital distribution. Each row of orbitals (Figure 3) can be classified as being predominantly “phen-like” (top row), “pyrazine-like” (middle row), or “quinone-like” (bottom row) by their similarity with the LUMOs of phen, pyrazine, and *para*-quinones, respectively. If we adopt a view of the ligands as assemblies of phen, pyrazine, and quinone acceptor components, then we can use the localized nature of the LUMOs discussed above to describe the excited state properties of these complexes as a series of electron-transfer reactions between the various components of the ligands. For example, tatpq can be viewed as an assembly of phen–pz–q–pz–phen (where pz indicates the pyrazine subunit and q indicates the quinone-based moiety) and tatpp as phen–pzphpz–phen (where pzphpz indicates the three central fused rings). This type of interpretation has previously been used to describe the excited-state properties of related tpphz (phen–pz–phen)<sup>6,10,11</sup> and dppz (phen–pz)<sup>9,12</sup> complexes and is quite useful for

**Table 1.** Spectroscopic and Redox Data for the New Complexes, in Deaerated Acetonitrile Unless Otherwise Stated, with the Relevant Data of the Closely Related Complexes **3** and **4** Also Reported for Comparison

compd	abs, 298 K: $\lambda_{\text{max}}$ , nm ( $\epsilon$ , $\text{M}^{-1} \text{cm}^{-1}$ )	lumin, 298 K: $\lambda_{\text{max}}$ , nm; $\tau$ , $\mu\text{s}$ ; $\Phi$	lumin, 77 K: <sup>a</sup> $\lambda_{\text{max}}$ , nm; $\tau$ , $\mu\text{s}$	redox, 298 K: oxidn; redn
<b>1</b> , [(phen) <sub>2</sub> Ru(tatpp)Ru(phen) <sub>2</sub> ] <sup>4+</sup>	443 (65 100) 323 (87 100) 261 (174 800)	no emission	no emission	+1.36 [2]; <sup>b</sup> -0.18 [1], -0.56 [1]
<b>2</b> , [(phen) <sub>2</sub> Ru(tatpq)Ru(phen) <sub>2</sub> ] <sup>4+</sup>	440 (33 800) 368 (42 750) 318 (47 850) 262 (158 650)	no emission	no emission	+1.37 [2]; -0.23 [1], -0.60 <sup>c</sup>
<b>3</b> , [(phen) <sub>2</sub> Ru(tpphz)Ru(phen) <sub>2</sub> ] <sup>4+</sup> <sup>d</sup> [(phen) <sub>2</sub> Ru(tpphz)] <sup>2+</sup> <sup>d</sup>	439 (35 900) 445 (18 500)	710; 0.1; $5 \times 10^{-3}$ 625; 1.2; $7 \times 10^{-2}$	583; 4.1 580; 5.9	+1.34 [2]; -0.78 [1] +1.34 [1]; -1.00 [1]

<sup>a</sup> In butyronitrile rigid matrix. <sup>b</sup>  $E_{1/2}$  values vs SCE are reported; the number in brackets refers to the number of exchanged electrons. Processes are reversible except otherwise stated. <sup>c</sup> Quasi-reversible process. <sup>d</sup> Data from ref 6.

interpreting the spectroscopic, photophysical, and redox data here.

Cyclic and differential pulse voltammetry experiments showed that, on oxidation, both **1** and **2** undergo a single bielectronic reversible process (Table 1). This suggests that the two metal-centered oxidations take place independently (i.e., the metal centers are only weakly interacting with one another). The oxidation potentials of the two complexes are very close to one another and also similar to that of the tpphz dimer **3** (+1.34 V),<sup>6</sup> as well as of similar dinuclear ruthenium complexes containing long fully aromatic bridging ligands.<sup>1c,f</sup>

On reduction, compound **1** undergoes two reversible reductions at -0.18 and -0.56 V consistent with complete population of the  $b_{3u}$  orbital and formation of the tatpp dianion. Differential pulse voltammetry further showed that the two reductions on **1** are each one-electron processes using the  $\text{Ru}^{2+/3+}$  peak as an internal standard. Successive reduction processes, most likely connected with first reduction processes of the peripheral phen ligands and successive reductions of the bridge, are observed at potential more negative than -1.2 V, but they are ill-behaved and are not discussed. The quinone complex **2** also undergoes two reductions (Table 1); however, only the first is reversible and the second is quasi-reversible. We suspect that these reduction processes lead to the formation of the hydroquinone dianion but can only confirm, at this juncture, that the first reduction is a one-electron process.

It is interesting to note that the tatpp complex **1** is easier to reduce than the tatpq complex and both new complexes, **1** and **2**, are easier to reduce than complex **3**, containing the tpphz bridging ligand (Table 1). These results are completely consistent with the PM3 orbital calculations of the relative energy levels of the  $b_{3u}$  (tatpp),  $b_{1g}$  (tatpq), and  $b_{3u}$  (tpphz) orbitals (see Figure 4) and suggest that the electrochemical process directly populates the LUMO for each complex, as expected.

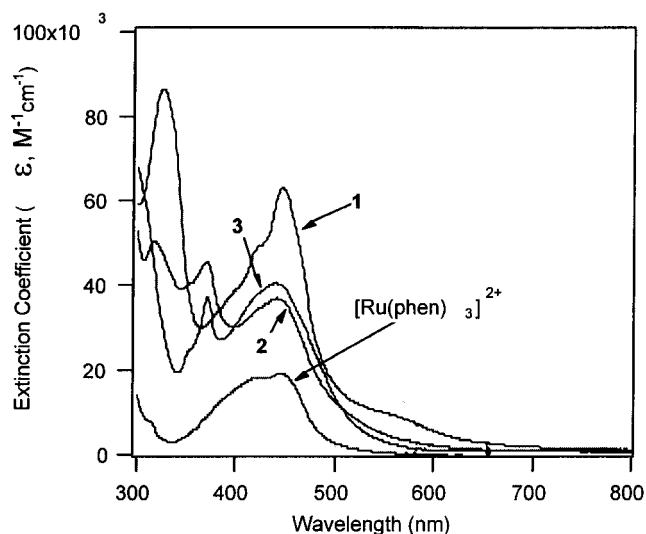


**Figure 5.** Absorption spectra of **1** (solid), **2** (dashed), **3** (dotted), and  $[\text{Ru}(\text{phen})_3]^{2+}$  (dot-dash) as the  $\text{PF}_6^-$  salts in acetonitrile solution.

The absorption spectra of **1** and **2** in acetonitrile solution are dominated by very intense spin-allowed ligand-centered (LC) transitions in the UV region and by intense spin-allowed metal-to-ligand charge-transfer (MLCT) transitions in the visible and are shown in Figure 5 (see also Table 1 for some relevant data). In particular, the bands around 440 nm for both the complexes are similar in energy and shape to the lowest-energy absorption band of  $[\text{Ru}(\text{phen})_3]^{2+}$ , which is assigned to the spin-allowed  $\text{Ru}(d\pi) \rightarrow \text{phen}(\pi^*)$  MLCT transition which upon intersystem crossing directly produces the triplet MLCT excited state which is responsible for the luminescent behavior of  $[\text{Ru}(\text{phen})_3]^{2+}$ .<sup>13</sup> As already pointed out for other oligonuclear polypyridine metal complexes containing bridging ligands with extended delocalization, the low-lying orbitals localized on the central portion of the bridging ligand are often decoupled from the metal  $t_{2g}$ -type orbitals<sup>6,10-12</sup> because they have little to no orbital contribution or inappropriate orbital symmetry on the nitrogens of the phenanthroline portions. Therefore, the remote MLCT transitions involving such low-lying orbitals essentially have small to negligible oscillator strengths. Of all the compounds with low-lying "bridge-centered" orbitals, only **1** shows an absorption at longer wavelengths (a moderately intense peak

- (10) (a) Bolger, J.; Gourdon, A.; Ishow, E.; Launay, J.-P. *Inorg. Chem.* **1996**, *35*, 2937. (b) Ishow, E.; Gourdon, A.; Launay, J.-P.; Lecante, P.; Verelst, M.; Chiorboli, C.; Scandola, F.; Bignozzi, C.-A. *Inorg. Chem.* **1998**, *37*, 3603. (c) Ishow, E.; Gourdon, A.; Launay, J.-P.; Chiorboli, C.; Scandola, F. *Inorg. Chem.* **1999**, *38*, 1504. (d) Chiorboli, C.; Bignozzi, C.-A.; Scandola, F.; Ishow, E.; Gourdon, A.; Launay, J.-P. *Inorg. Chem.* **1999**, *38*, 2402
- (11) Flamigni, L.; Encinas, S.; Barigelletti, F.; MacDonnell, F. M.; Kim, M.-J.; Puntoriero, F.; Campagna, S. *Chem. Commun.* **2000**, 1185.
- (12) Chambron, J.-C.; Sauvage, J.-P.; Amouyal, E.; Kiffi, P. *Nouv. J. Chim.* **1985**, *9*, 527.

- (13) Juris, A.; Balzani, V.; Barigelletti, F.; Campagna, S.; Belser, P.; von Zelewsky, A. *Coord. Chem. Rev.* **1988**, *84*, 85 and references therein.

at 580 nm) which may be due to a direct  $t_{2g} \rightarrow b_{3u}$  MLCT transition. The main contributions to the bands around 440 nm can therefore be safely assigned to a combination of  $t_{2g} \rightarrow a_2$  (Ru  $\rightarrow$  phen) and  $t_{2g} \rightarrow a_u$  (Ru  $\rightarrow$  tatpp (**1**); Ru  $\rightarrow$  tatpq (**2**)) CT transitions.

It is clear that for **1** the band at 440 nm also receives contributions from a LC ( $\pi \rightarrow \pi^*$ ) transition involving the bridging ligand. This is indicated by the significantly higher extinction coefficient of the band in **1** compared to that in **2** or **3** (Table 1 and Figure 5) and from its structured shape. Interestingly, a similarly structured band, blue-shifted with respect to that of **1** (peaking at about 380 nm), is observed in both **2** and in oligonuclear Ru complexes containing tpphz (including **3**).<sup>6,10,11</sup> This absorption has been assigned to LC transitions for the tpphz ligand<sup>10a</sup> and is similarly associated with a LC absorption in tatpq. This trend correlates well with the relative HOMO–LUMO gaps calculated for tatpp (6.0 eV), tatpq (7.4 eV), and tpphz (7.3 eV) for the free ligands.

The two new dimers **1** and **2** are not luminescent (for excitation wavelengths between 320 and 480 nm) both at room temperature in acetonitrile solution and at 77 K in a butyronitrile rigid matrix, contrary to what was found for **3**.<sup>6,10,11</sup> This indicates that efficient quenching of the (inherently emissive) Ru  $\rightarrow$  phen CT excited state takes place in **1** and **2**. To understand the origin of the quenching, it is useful to recall that Ru  $\rightarrow$  phen CT emission was quenched in **3** at room temperature in fluid solution by almost isoergonic electron transfer from the excited chromophore directly formed by 440 nm light excitation (where the promoted electron is essentially localized on a phenanthroline-based orbital) to the pyrazine-based moiety of the bridge,<sup>14</sup> with generation of a charge-separated species which is also luminescent, although with a significantly reduced quantum yield.<sup>6,11,15</sup> The rate constant of such an electron-transfer process in **3** in dichloromethane is around  $5.0 \times 10^9 \text{ s}^{-1}$  and becomes at least 1 order of magnitude larger in acetonitrile, where the charge-separated state is stabilized.<sup>11</sup> For **3**, the electron-transfer process was hampered at 77 K in rigid glasses because of nonnegligible energy barriers.<sup>6</sup> For the two new dimers, the driving forces (at room temperature in acetonitrile)<sup>15</sup> for electron transfer from the excited chromophore to the pzphz ( $b_{3u}$ ) moiety of **1** and to the quinone ( $b_{1g}$ ) moiety of **2** are much larger at  $-0.60$  and  $-0.55$  eV, respectively, as determined from redox data and by taking the high-energy feature of the 77 K emission spectrum of  $[(\text{phen})_2\text{Ru}(\text{tpphz})]^{2+}$  as the excited-state energy of the Ru(II)-based chromophore (2.14 eV).<sup>6</sup> Even consider-

ing the longer distance between the electron-transfer partners in **1** and **2** with respect to that in **3**, the calculated electron-transfer driving forces can justify faster processes and quantitative quenching even at 77 K. So we suggest that electron transfer from the Ru  $\rightarrow$  phen CT excited state to the central bridge moieties could be held responsible for the quantitative quenching of the Ru  $\rightarrow$  phen CT emission in **1** and **2** both at room temperature and at 77 K.<sup>16</sup> A very similar situation has been observed for Re(I) complexes of the aqphen ligand (Figure 1).<sup>2c</sup> Two ligand-based  $\pi$ -accepting orbitals, one phenazine-based and one quinone-based, are found at energies lower than that of the phenanthroline  $\pi^*$  orbital. Luminescence quenching in this case is shown to the result of intramolecular electron transfer to the orbital largely centered on the quinone portion of the ligand. It should be noted that the presence of low-lying triplet excited states localized within the bridging ligands cannot be excluded. Such excited states could quench the MLCT luminescence of the external metal-based subunits by energy-transfer processes; however, at this stage there is no simple way to investigate this point. We still favor the electron-transfer hypothesis because the bridging ligand centered excited states should give rise to luminescence, at least at 77 K, contrary to the experimental data.

In conclusion, we have described two new dinuclear Ru(II) polypyridine complexes containing large aromatic bridging ligands and have found that subunits of these bridging ligands may behave as individual components affecting the photo-physical properties of the Ru-based chromophores as a whole. In particular, MLCT emission is efficiently quenched at room temperature and at 77 K, most likely by exoergonic electron-transfer processes involving bridging ligand subunits. We view these results as significant for the rational design of large systems with useful photo- and redox-driven properties.

**Acknowledgment.** This work was supported by the MURST EC-TMR Program (S.C., Contract No. FMRX-CT-980226), U.S. National Science Foundation Grants (CHE-0101399 (F.M.M.); CHE-9876249 (G.K.)), and the Robert A. Welch Foundation (F.M.M.).

**Supporting Information Available:** <sup>13</sup>C NMR, MALDI mass spectrometry, cyclic voltammetry, and HOMO orbital data for **1** and **2**. This material is available free of charge via the Internet at <http://pubs.acs.org>.

IC011028U

(14) This electron-transfer process could be viewed as a nonradiative  $a_u \rightarrow b_{3u}$  electronic transition.

(15) The driving force of the processes was calculated in a first approximation by the equation  $\Delta G = e[E_{\text{ox}}^* - E_{\text{red}}]$ , where  $e$  is the electron charge,  $E_{\text{red}}$  is the ground-state reduction potential, and  $E_{\text{ox}}^*$  is the oxidation potential of the excited state,  $E_{\text{ox}}^* = E_{\text{ox}} - E_{00}$ , where  $E_{\text{ox}}$  is the oxidation potential of the ground state and  $E_{00}$  is the energy level of the excited state. The entropy factor and work term are neglected.

(16) Electron transfer from an excited Ru(II)-based chromophore to a quinone moiety covalently linked to a coordinating bpy by an ethylene chain has been reported to take place with a rate constant of  $1.0 \times 10^{10} \text{ s}^{-1}$ ;<sup>17</sup> however, this result is difficult to compare with the results obtained for **2** because the driving forces are different. The quinone moiety in tatpq, although maintaining its identity, is expected to be influenced by its environment (the geometry of the complexes are significantly different) and, in fact, is reduced at a less negative potential than the bpy-substituted quinone ( $-0.23$  vs  $-0.44 \text{ V}^{17}$ ).

(17) Gouille, V.; Harriman, A.; Lehn, J.-M. *J. Chem. Soc., Chem. Commun.* **1993**, 1034.